International Journal of Naval Architecture and Ocean Engineering 13 (2021) 187–193

Contents lists available at ScienceDirect

International Journal of Naval Architecture and Ocean Engineering

journal homepage: http://www.journals.elsevier.com/international-journal-of-naval-architecture-and-ocean-engineering/

Seafloor terrain detection from acoustic images utilizing the fast two-dimensional CMLD-CFAR

Jiaqi Wang [a, b, c], Haisen Li [a, b, c], Weidong Du [a, b, c, *], Tianyao Xing [a, b, c], Tian Zhou [a, b, c]

[a] Acoustic Science and Technology Laboratory, Harbin Engineering University, Harbin, China
[b] Key Laboratory of Marine Information Acquisition and Security (Harbin Engineering University), Ministry of Industry and Information Technology, Harbin, China
[c] College of Underwater Acoustic Engineering, Harbin Engineering University, Harbin, China

ARTICLE INFO

Article history:
Received 18 November 2019
Received in revised form
20 October 2020
Accepted 18 November 2020

Keywords:
Seafloor terrain detection
Two-dimensional censored mean level detector-constant false alarm rate
Multi-beam echo sounder

ABSTRACT

In order to solve the problem of false terrains caused by environmental interferences and tunneling effect in the conventional multi-beam seafloor terrain detection, this paper proposed a seafloor topography detection method based on fast two-dimensional (2D) Censored Mean Level Detector-statistics Constant False Alarm Rate (CMLD-CFAR) method. The proposed method uses s cross-sliding window. The target occlusion phenomenon that occurs in multi-target environments can be eliminated by censoring some of the large cells of the reference cells, while the remaining reference cells are used to calculate the local threshold. The conventional 2D CMLD-CFAR methods need to estimate the background clutter power level for every pixel, thus increasing the computational burden significantly. In order to overcome this limitation, the proposed method uses a fast algorithm to select the Regions of Interest (ROI) based on a global threshold, while the rest pixels are distinguished as clutter directly. The proposed method is verified by experiments with real multi-beam data. The results show that the proposed method can effectively solve the problem of false terrain in a multi-beam terrain survey and achieve a high detection accuracy.

1. INTRODUCTION

Multi-Beam Echo Sounder (MBES) is one of the most important high-tech marine survey equipment in the contemporary marine survey field. The MBES has been widely used in hydrographic surveys, oceanographic engineering, exploration, development of seafloor resources, and other fields (Ferrini, 2004; Jung et al., 2018; YuZhe et al., 2017). The robustness of multi-beam seafloor terrain detection technology is directly related to the reliability of detection results. According to relates studies, the main factors influencing the robustness of the multi-beam bathymetric technology are sounding artifacts and outliers. The most typical sounding artifact is the tunneling effect (De MoustierMartin, 1986). As a consequence, it poses a challenge to detect seafloor terrain robustly and efficiently.

When measured seafloor has strong reflexes, the side lobe will leak into other beams due to the strong energy of the mirror beam, thus causing a strong interference to the lateral beam. When the side lobe response is higher than the system detection threshold, the system will track the side lobe response and ignore the true seafloor echo, thus causing a tunneling effect in measurement results (Kammerer, 2000; Du et al., 2016; Alexandrou and de Moustier, 1988). Namely, when an initial image is transformed into the final seafloor terrain image by sector-transforming, the lateral interference becomes circular, and its shape is close to the tunnel's shape, which is why it is called the tunneling effect. In conventional multi-beam data processing, post-processing software is often used to manually erase the outliers. However, when there are many surveying lines, and when the scope of surveying is large, this method has a huge workload and is a highly subjective factor. Therefore, it is very important to solve the problem of false terrain in multi-beam seafloor terrain detection. Wei et al. (Yukuo et al., 2011; Wei et al., 2010) researched the multi-beam false terrain removal method from the aspects of reducing the side lobe. In (Yukuo et al., 2011; Wei et al., 2010), the MVDR beam-forming algorithm and the recursive least square-Laguerre lattice algorithm were used to reduce the side lobe interference, thus

* Corresponding author.
E-mail address: wangjiaqi@hrbeu.edu.cn (W. Du).
Peer review under responsibility of The Society of Naval Architects of Korea.

https://doi.org/10.1016/j.ijnaoe.2020.11.004

eliminating the tunneling effect. However, the above algorithms have high computational cost and are severely limited in practical applications. In order to enhance the practicability of the algorithm, Chen et al. (2010) proposed a fast algorithm based on apFFT, but the actual effect was not satisfactory.

The CFAR technology has been proven to have an excellent ability to control false alarm in the background that obeys the Gaussian distribution. Typical CFAR techniques are the Cell Averaging-Constant False Alarm Rate (CA-CFAR) and the Order Statistics-Constant False Alarm Rate (OS-CFAR) (Rohling, 1983; Gao et al., 2009; Boudemagh et al., 2014). With the continuous development of the CFAR technology, this technology has been widely applied in the field of sonar technology (Acosta and Villar, 2015; Villar et al., 2013, 2017). In the aspect of multi-beam image processing, Gao et al. (2017) proposed a subset censored CFAR method for a multi-target environment, but the processing effect in a continuous expansion target environment was not ideal. In the 2D CFAR detection, due to a large number of pixels and reference cells, the computation amount of the traditional algorithm is large, which limits its application in practice (Kronauge and Rohling, 2013). In order to address this problem, the practicality of the CFAR detection method has been improved by reducing the parameter estimation calculation amount and the number of measured pixels (Gao et al., 2006; Tao et al., 2016). Motivated by the results of related studies and aiming to solve the current problems in multi-beam seafloor terrain target detection, this paper proposes a fast 2D Censored Mean Level Detector - Constant False Alarm Rate (CMLD-CFAR) method for multi-beam seafloor terrain target detection.

The rest of the paper is organized as follows. In Section 2, the 1D CA-CFAR algorithm is discussed and extended to 2D, the influence of the sliding window size on parameter estimation is analyzed, and a fast 2D CMLD-CFAR method based on a global threshold, which overcomes the disadvantages of the traditional detection algorithm, is proposed. In Section 3, the effectiveness of the proposed method is verified, and the processing performances of different CFAR methods are compared at different sliding windows. In Section IV, the main conclusions are drawn.

2. Detection method based on fast 2D CMLD-CFAR

2.1. CA-CFAR principle

The tunneling effect makes the Weighted Mean Time (WMT) sounding method experience the side lobe interferences caused by a strong echo signal in the terrain echo signal, which results in an incorrect terrain detection. In the field of radar signal processing, in order to adapt to a constant change in the interference level, the CFAR detection technology is generally used to predict detection threshold and reduce the probability of false alarm in the actual interference environment, which is known as adaptive threshold detection technology or automatic detection technology. The processing flowchart of the typical CA-CFAR algorithm is shown in Fig. 1.

The clutter power in the CA-CFAR algorithm is estimated based on the mean value of reference cells nearby the Cell Under Test (CUT). In the case of clutter following the Gauss distribution, this is the maximum likelihood estimation. Assume αdenotes a scalar multiple, which can be calculated by the presupposed false alarm probability and the number of reference cells.

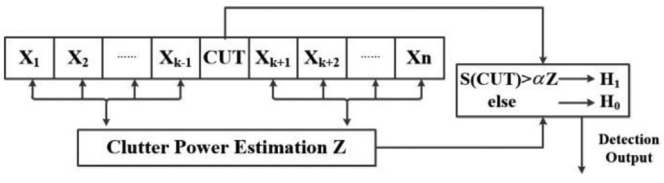

Fig. 1. The flowchart of 1D CFAR progressing.

The reference cells of every CUT can be represented by a set of vectors $X = (x_1, x_2, \ldots, x_n)$. Another assumption is that each reference cell is independently and identically distributed (i.i.d.), so the joint probability distribution function of the reference cells can be expressed as:

$$f(X) = \prod_{i=1}^{N} f(x_i) \tag{1}$$

The determining procedure of the detection threshold is given below. In the MBES acoustic images processing, an exponential distribution is often used to express the Probability Density Function (PDF) of images, and the PDF of each CUT can be expressed as:

$$f(x) = \frac{1}{\beta^2} e^{-x/\beta^2} \tag{2}$$

where x represents the amplitude of the CUT, and $x > 0$; denotes the average clutter power, and its estimation is given by (Acosta and Villar, 2015):

$$\beta^2 = \frac{1}{N}\sum_{i=1}^{N} x_i \tag{3}$$

where N denotes the number of reference cells. In order to obtain the constant false alarm rate, the adaptive threshold T can be expressed as:

$$T = \alpha\beta^2 = \frac{\alpha}{N}\sum_{i=1}^{N} x_i \tag{4}$$

by *substituting* Eq. (4) into Eq. (1), we get:

$$f(X) = \prod_{i=1}^{N} \frac{1}{\beta^2} e^{-x_i/\beta^2} = \frac{1}{\beta^{2N}} e^{-\frac{1}{\beta^2}\left(\sum_{i=1}^{N} x_i\right)}. \tag{5}$$

A false alarm happens when a Cell Under Test (CUT) exceeds threshold T, so the false alarm probability can be expressed by:

$$P_{fa} = \int_0^{\infty} P(CUT > T) \cdot f(X) dX \tag{6}$$

By substituting Eq. (2) and Eq. (5) into Eq. (6), we have:

$$P_{fa} = \prod_{i=1}^{N} \int_0^{\infty} e^{-(1+(\alpha/N))x_i} dx_i = \left(1 + \frac{\alpha}{N}\right)^{-N} \tag{7}$$

By settling the Eq. (7), a multiple α of the adaptive threshold is obtained as follows:

$$\alpha = N \cdot \left(P_{fa}^{-\frac{1}{N}} - 1\right) \tag{8}$$

Thus, when multiple α and the number of reference cells are determined, the false alarm probability P_{fa} can be obtained, i.e., the CFAR detection is completed.

2.2. 2D CMLD-CFAR method

In the field of image processing, interferences are usually distributed around the targets. The reference cells of a traditional CFAR detector contain only a one-dimensional signal, which can result in an inaccurate estimation of the clutter power level and affect the false alarm rate. In the MBES terrain detection, an initial terrain image is two-dimensional, where the abscissa denotes the beam angle, and the ordinate denotes the distance. Accordingly, this paper extends the traditional one-dimensional CFAR algorithm into a two-dimensional CFAR algorithm to increase the number of reference cells and control the false alarm probability effectively.

The commonly used two-dimensional sliding windows are shown in Fig. 2, which are mainly divided into rectangular windows and cross-sliding windows. Guard cells are used to avoid the interference of a target. In the following, N_r and N_g represent the numbers of sliding reference cells and guard cells, respectively. In this paper, $N_r = 100$ and $N_g = 50$. A rectangular window contains more reference cells than a cross window, and a cross window includes adjacent reference cells of a CUT only in a positive direction. The false alarm rate control capabilities of the two window types can be obtained by analyzing the estimated clutter power corresponding to different CUTs. The estimations obtained using different sliding windows of typical CUTs presented in Fig. 5(a) are given in Table 1. The data in Table 1 denote the clutter power level estimations obtained by averaging the references with different sliding windows.

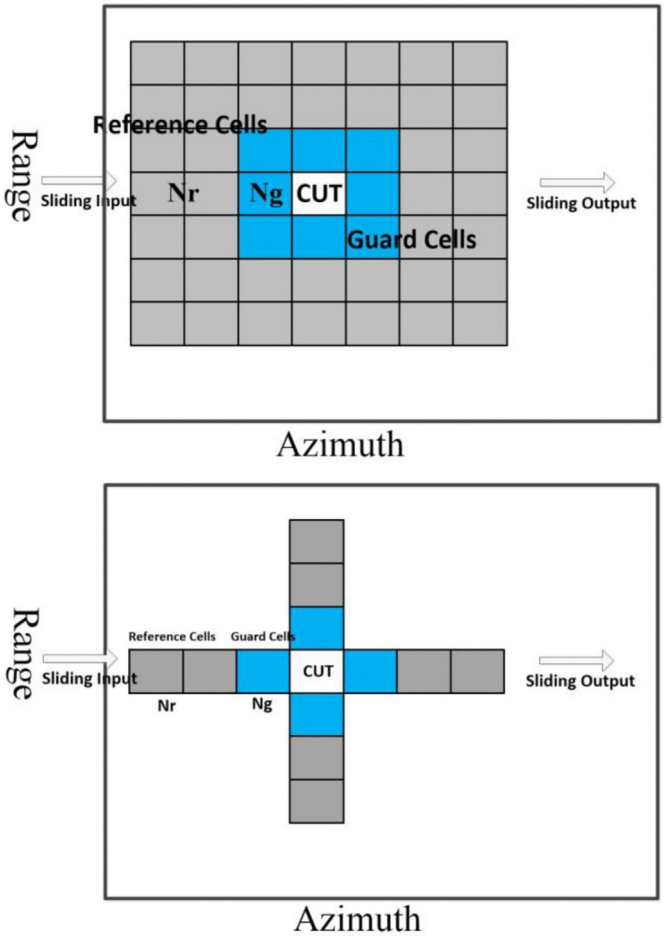

Fig. 2. The 2D CFAR with a sliding window.

Table 1
ESTIMATIONS FOR DIFFERENT SLIDING WINDOWS.

Serial number	Estimations of different sliding windows	
	Rectangular window	Cross window
1	2608	3594
2	3778	5409
3	2507	3395

As shown in Table 1, the clutter power level estimated using the rectangular window is much smaller than the estimates obtained using the cross-sliding window, which results in an increase in the false alarm probability. Because of the directivity and the side lobe of the beam-forming algorithm, the main interferences, such as the tunneling effect, are usually distributed in the vertical and horizontal directions of the targets. So, as shown in Table 1, the cross-sliding windows can provide a more suitable and higher threshold. Therefore, this paper uses a cross-sliding window for terrain detection. The effects on actual data processing of different sliding windows are analyzed in Section 3.

Under the condition of the Gaussian background clutter, the CFAR detector can provide constant false alarm detection. However, in the real multi-beam terrain data processing, the CA-CFAR algorithm can difficultly achieve the theoretical detection performance due to clutter heterogeneity. The OS-CFAR method estimates the clutter power level by sorting the reference cells and taking the value at a specific location as an estimation. This method is convenient for multi-target environments. Since the targets in a seafloor terrain image are numerous and relatively dense, there are usually many strong target interferences in reference cells. Therefore, this paper uses the 2D CMLD-CFAR algorithm to detect the target to control the false alarm rate. The diagram of the 2D CMLD-CFAR algorithm is shown in Fig. 3.

The target occlusion phenomenon that occurs in the multi-target environment can be eliminated by censoring large reference cells, and the remaining reference cells are used to calculate the local threshold. The algorithm discards large reference cells and takes the mean of the remaining reference cells as an estimate of the clutter power level, which is different from the CA-CFAR algorithm.

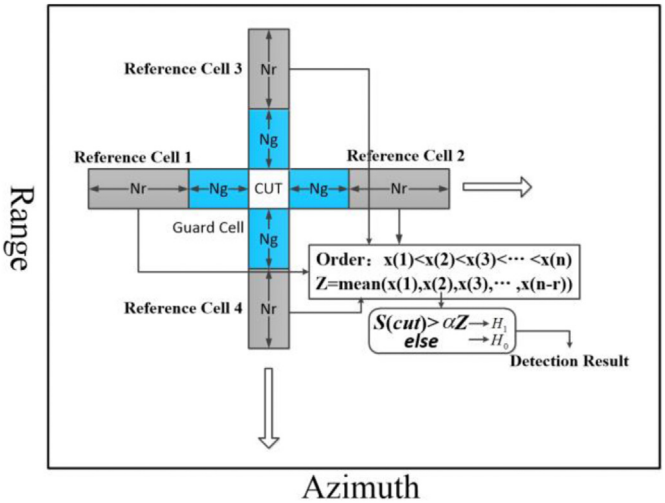

Fig. 3. The diagram of the 2D CMLD-CFAR with a cross-sliding window.

$$\beta^2 = \frac{1}{4N_r}\sum_{i=1}^{4N_r-r} x_i \tag{9}$$

where $N = 4N_r$ and $r = 15$, and r denotes the number of large reference cells that are censored.

In order to get the false alarm probability of the CMLD detection method, a linear transformation is conducted on the remaining reference cells.

$$\begin{aligned} Z &= \sum_{i=1}^{N-r} x_i = \sum_{i=1}^{N-r} v_i \\ v_i &= (N-r-i+1)(x_i - x_{i-1}), x_0 = 0 \end{aligned} \tag{10}$$

and the PDF of v can be expressed as:

$$\begin{aligned} f(v_i) &= \frac{c_i}{\mu} e^{-c_i v_i/\mu} \\ c_i &= \frac{N-i+1}{N-r-i+1} \end{aligned} \tag{11}$$

By substituting Eq. (10) into Eq. (11), we get:

$$\begin{aligned} f(Z) &= \sum_{i=1}^{N-r} \frac{a_i}{\mu} e^{-c_i z/\mu} \\ a_i &= \binom{N}{r}\binom{N-r}{i-1}(-1)^{i-1}\left(\frac{N-i+1-r}{r}\right)^{N-r-1} \end{aligned} \tag{12}$$

By substituting Eq. (11) and Eq. (12) into Eq. (6), the false alarm probability can be obtained as:

$$P_{fa} = \sum_{i=1}^{N-r} \frac{a_i}{c_i + T} \tag{13}$$

2.3. Fast algorithm

Even if the calculation amount of the parameter estimation in the CFAR algorithm is small, when there are too many pixels in acoustic images, excessive computational and time resources will be required for applying the proposed method to a whole acoustic image sequence. By analyzing an actual multi-beam seafloor terrain image, it can be concluded that in the image, many pixels are obviously not targets. Therefore, this paper proposes a fast algorithm based on a global threshold to extract the region of interest (ROI) in an image. Only the Regions of Interest (ROI) that are selected according to a global threshold are detected by the 2D CMLD-CFAR method, and the remaining pixels are directly distinguished as clutter. The global threshold can be expressed as:

$$T_G = \frac{L}{N_t}\sum_{i=1}^{N_t} x_i \tag{14}$$

where L denotes the threshold level and can be selected as the amount of computation load; N_t denotes the total number of pixels in a sonar image. Thus, the global threshold can be regarded as a product of the overall average amplitude of an image at the threshold level. If a pixel value is larger than the global threshold, the pixel is regarded as the ROI; otherwise, it is regarded as the clutter directly.

Table 2
NUMBERS OF ROI PIXELS.

Level of threshold L	Global threshold level				
	1	2	3	4	5
Number of ROI pixels	1,062,905	459,107	211,464	117,492	79,796
Total number of pixels	511,500 [5000 1023]				

As shown in Table 2, for the total number of pixels obtained from Fig. 5, the number of ROI pixels is far less than the total prime number for levels 4 and 5. Considering the computational load and detection performance at the same time, this paper sets the threshold to level 4.

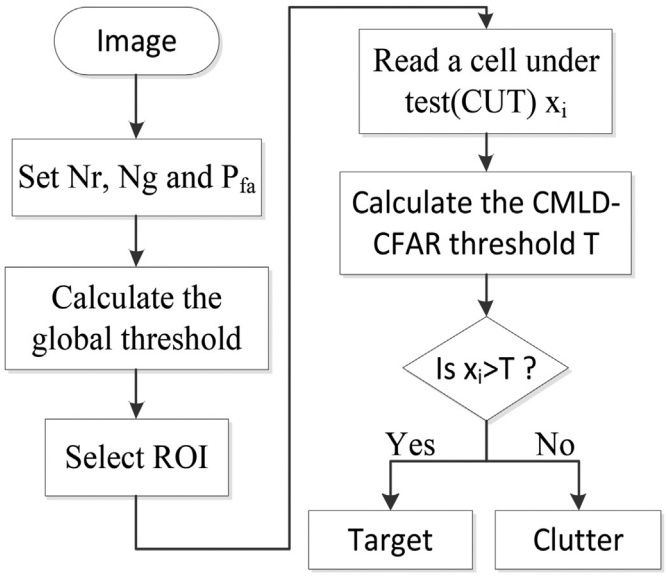

Fig. 4. The flowchart of the 2D CMLD-CFAR method.

2.4. Overview of the proposed method

The entire processing flowchart of the fast 2D CMLD-CFAR method is shown in Fig. 4.

The main steps of the proposed method can be summarized as

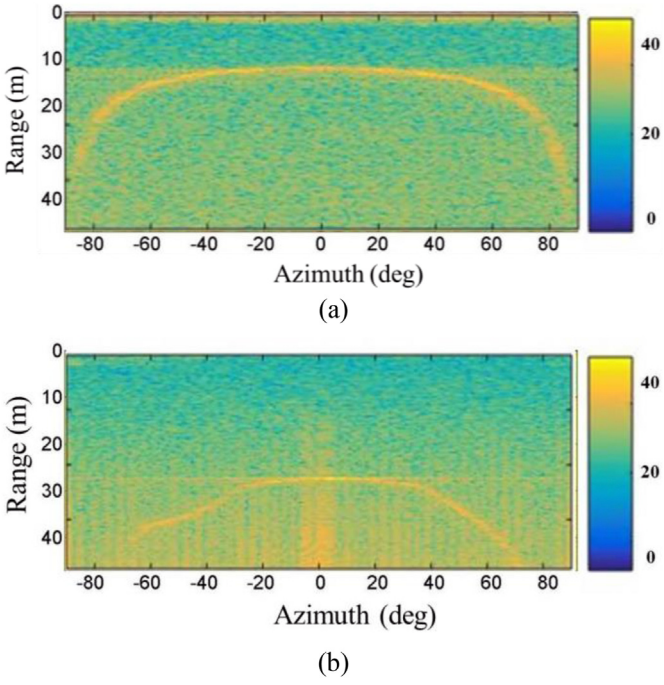

Fig. 5. The multi-beam initial seafloor terrain view.

follows:

- Select the number of reference cells N_r, the number of guard cells N_g, and set the false alarm rate P_{fa};
- Calculate the global threshold, determine the ROI, and label the remaining area as the background clutter;
- Detect the ROI and estimate the threshold T corresponding to the CUT;
- Compare the CUT with the corresponding local thresholds; the CUT is determined to be part of the target when $S\ (cut) > T$; otherwise, it is considered to be the background;

3. Experimental results

3.1. Data description

The data used in the experiments were measured in the typical waters of the Songhua Lake in Jilin City, Jilin Province, China, by the multi-beam sonar developed by Harbin Engineering University. The sonar system emitted a Continuous-Wave (CW) signal at a frequency of 300 kHz. The multi-beam echo sounder had a linear array consisting of 64 elements. For the sake of easy processing, the initial seafloor terrain image was used in the 2D CMLD-CFAR detection. The typical initial seafloor terrain image is shown in Fig. 5. All the seafloor terrains were natural. The continuous strip-like area in the image denoted the seafloor terrain target, and the remaining part of the image denoted the interference clutter.

3.2. Results and comparisons

Two typical multi-beam seafloor terrain images are presented in Fig. 5(a) and (b). The initial seafloor terrain images were formed by the orthogonal method and the Fourier Transform (FT) beamforming. The average depths of the terrain in Fig. 5(a) and (b) are about 20 m and 45 m, respectively.

The processing results obtained using different sliding windows are presented in Fig. 6. As shown in Fig. 6(a) and (b), when the 2D rectangular window was used to detect the terrain target, the reference cells in the rectangular window included not only strong correlation interference in the direction of the target but also the weak interference in other directions, so the estimation of the clutter power was low, resulting in a high false alarm rate; there were many outliers in the result, and the method failed to eliminate the tunneling effect. When the 1D transverse window was used, the

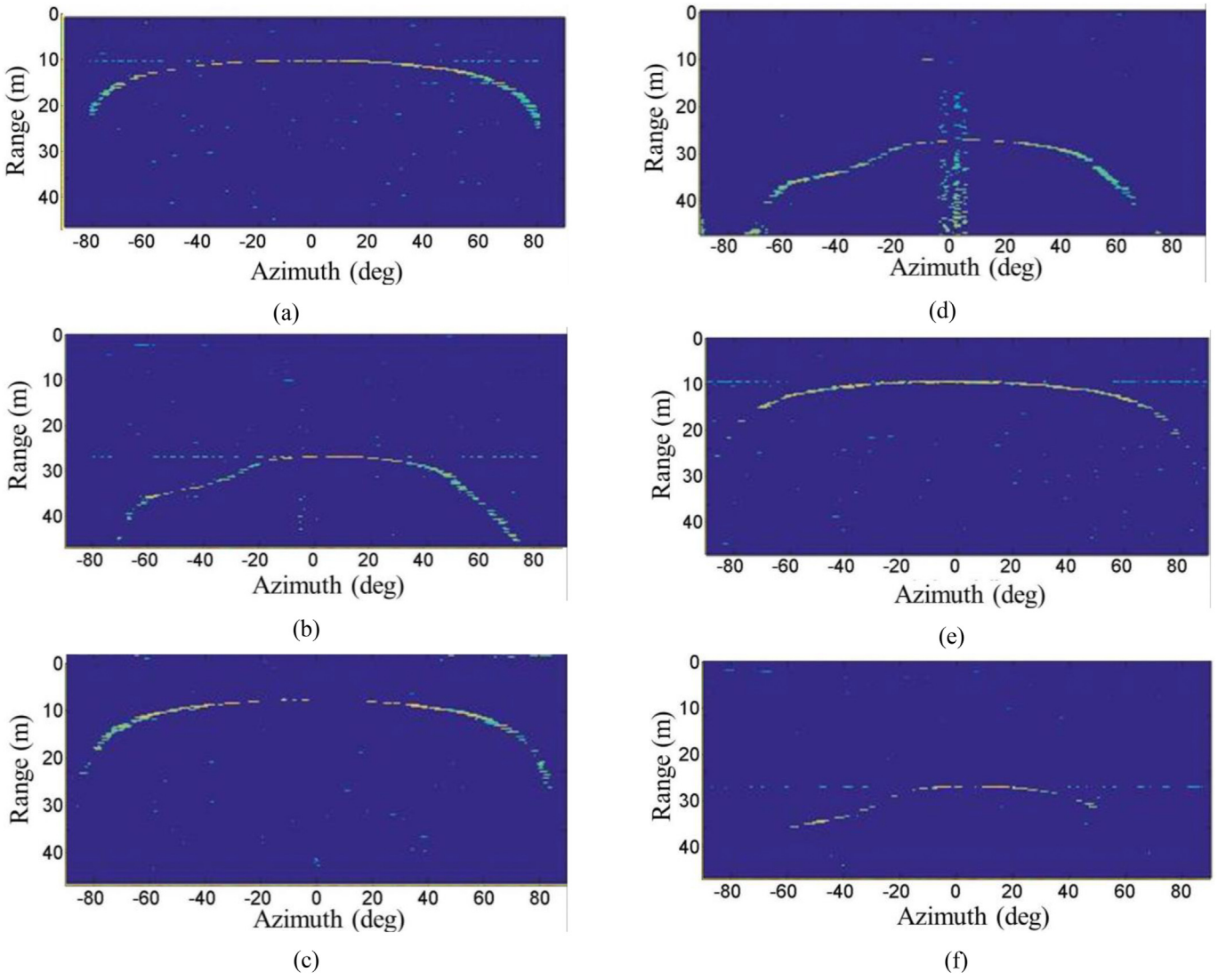

Fig. 6. Results for different sliding windows. (a) (b) Results for 2D rectangular window, (c) (d) Results for 1D transverse window, (e) (f) Results for 1D longitudinal window.

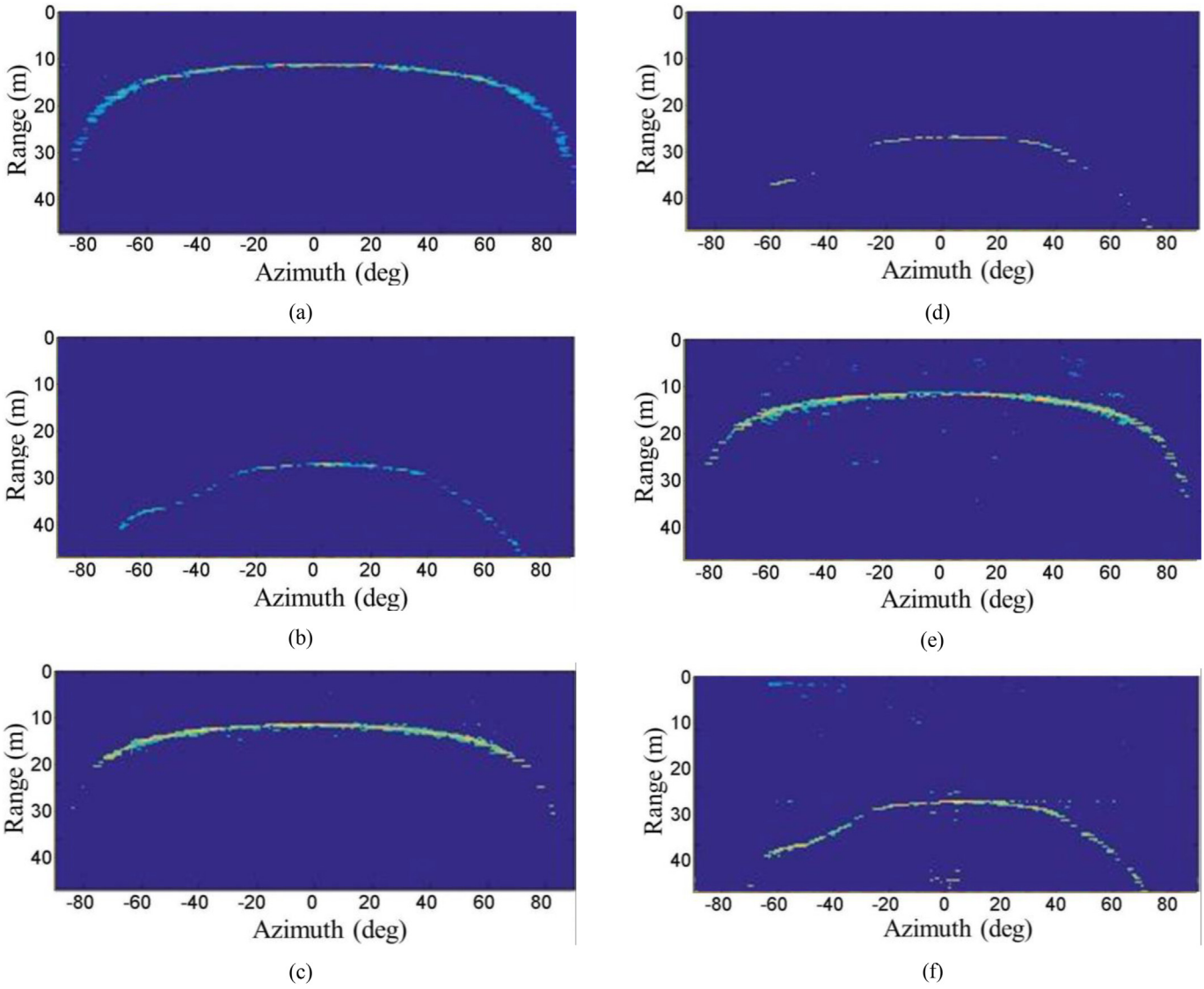

Fig. 7. Detection results of different methods with the cross-sliding window. (a) (b) Results of fast 2D CMLD-CFAR, (c) (d) Results of 2D CA-CFAR, (e) (f) Results of 2D OS-CFAR.

transverse reference cells included mainly side lobe interference, so the CFAR method based on the transverse could effectively solve the tunneling effect, as shown in Fig. 6(c) and (d). However, when the CUT was located in the middle area of the terrain, the interference of the center beam was too strong, resulting in the threshold higher than the normal clutter power, so the leakage alarm occurred. In Fig. 6(d), the center beam energy is high; the CFAR method based on the transverse window did not take into account the longitudinal interference information of the target, so there were a large number of false alarms in the strong beam region. The results for the 1D longitudinal window are shown in Fig. 6(e) and (f). Similar to results in Fig. 6(a) and (b), because the 1D longitudinal window did not consider beam side lobe interference, it was impossible to solve the artifact with accurate elimination of the tunneling effect. Therefore, the cross-sliding windows are more suitable for seafloor terrain detection in real multi-beam data.

Fig. 7 shows the results obtained by different CFAR methods. The results obtained by the 2D CMLD-CFAR method are presented in Fig. 7(a) and (b), where it can be seen that the proposed method could both achieve high accuracy in the seafloor terrain target detection in the multi-beam terrain image and control the false alarm rate effectively. The results obtained by the CA-CFAR are presented in Fig. 7(c) and (d). Because this method did not discard a part of the reference cells that might be the target interference, there was a low false alarm rate. Due to the existence of a large number of continuous targets in the multi-beam seafloor terrain image, a large number of leaks occurred, which resulted in partial missing of the final seafloor topographic map and affected the trust of the overall seabed topographic map. Particularly, as shown in Fig. 7(d), most of the terrain in the image was erroneously detected as clutter due to the low signal-to-noise ratio. Also, as shown in Fig. 7(c), the edge beam area also had a leak condition due to the low signal-to-noise ratio. The results obtained by the 2D OS-CFAR

Table 3
Average execution times of different methods.

Image	Execution time *t*, s		
	2D CA-CFAR	2D OS-CFAR	Fast 2D CMLD-CFAR
Fig. 5(a)	50.794	56.354	3.674
Fig. 5(b)	48.978	53.856	3.346

method are presented in Fig. 7(e) and (f). The OS-CFAR method has proven to be an effective detection method in multi-target situations. However, due to the complex interference environment of the real data, although the OS-CFAR could effectively remove the tunneling effect in the terrain image, there were also many false alarms, which affected the data processing performance. The experimental results show that the proposed 2D CMLD-CFAR method can perform well in multi-beam terrain detection.

The comparison of the execution times of different methods is given in Table 3. Since most pixels were filtered out by global thresholds, the processing time of the proposed method was obviously shorter than those of the other methods. Consequently, the proposed method can greatly reduce the processing time, which is highly valuable in real-time engineering applications.

4. Conclusion

In this paper, a seafloor terrain detection method is proposed. In the proposed method, the CMLD-CFAR strategy based on a 2D cross-sliding window is adopted, and the fast algorithm based on a global threshold is used to improve the processing speed. The main conclusions are as follows: (1) compared with the 1D sliding window and 2D rectangular-sliding window, the cross window is more suitable for the multi-beam terrain detection because it can effectively eliminate the tunneling effect and other strong interference; (2) terrain targets are directly connected with each other; by censored some of the large suspected reference cells, the CMLD-CFAR strategy can improve the detection rate while ensuring the false alarm rate, especially in areas with a low signal-to-noise ratio, such as edge beams; (3) the proposed method first uses a global threshold to screen images, and then determines the ROI in an image and performs accurate CFAR detection, while the remaining part of the image is directly identified as clutter. The proposed method is verified by experiments and compared with other detection methods. The results show that the proposed method can greatly reduce the number of pixels needed for accurate CFAR detection, thus reducing the computational load significantly. Due to the non-uniformity and particularity of the interference distribution in multi-beam acoustic images, it is difficult to simulate the images accurately and meaningfully. In this paper, the real multi-beam data of different cases are processed, and different sliding windows and detection strategies are analyzed and compared. The results show that the proposed 2D CMLD-CFAR method can effectively solve the problem of false terrain in a multi-beam terrain survey and achieve a high detection accuracy.

Declaration of competing interest

The authors declare that they have no known competing financial interests or personal relationships that could have appeared to influence the work reported in this paper.

Acknowledgements

The funders are National Key R&D Program of China (2017YFC0306000, 2016YFC1402303), National Natural Science Foundation of China (NSFC) (U1809212, U1709203, 41576102).

References

Acosta, Gerardo G., Villar, Sebastián A., 2015. Accumulated CA–CFAR process in 2-D for online object detection from sidescan sonar data. IEEE J. Ocean. Eng. 4 (13), 558–569.
Alexandrou, Dimitri, de Moustier, Christian, 1988. Adaptive noise canceling applied to sea beam sideloe interference eejection. IEEE J. Ocean. Eng. 13 (2), 70–76.
Boudemagh, Naime, Vitae, Author, Hammoudi, Zoheir, Vitae, Author, 2014. Automatic censoring CFAR detector for heterogeneous environments. AEU - Int. J. Electron. Commun. 68 (12), 1253–1260.
Chen, B., Li, H., Wei, Y., Yao, B., October 2010. Tunnel effect elimination in multi beam bathymetry sonar based on ap FFT algorithm. In: Proceedings of the IEEE 10th International Conference on Signal Processing (ICSP '10), pp. 2391–2394. Beijing, China.
De Moustier, Christian, Martin, C. Kleinrock, 1986. Bathymetric artifacts in Sea Beam data: how to recognize them and what causes them". J. Geophys. Res. 91 (B3), 3407–3424.
Du, Weidong, Zhou, Tian, Li, Haisen, Chen, Baowei, Wei, Bo, 2016. ADOS-CFAR algorithm for multibeam seafloor terrain detection. Int. J. Distributed Sens. Netw. 12 (8).
Ferrini, Vicki Lynn, 2004. Dynamics of Nearshore Sedimentary Environments Revealed through the Analysis of Multibeam Sonar Data. State University of New York.
Gao, Gui, Jiang, Yong-Mei, Zhang, Qi, Gang-Yao, Kuang, De-Ren, Li, 2006. Fast acquirement of vehicle targets from high-resolution SAR images based on combining multi-feature. Acta Electron. Sin. 34 (9), 1663–1667.
Gao, G., Liu, L., Zhao, L.J., Shi, G.T., Kuang, G.Y., 2009. An adaptive and fast CFAR algorithm based on automatic censoring for target detection in high-resolution SAR images. IEEE Trans. Geosci. Rem. Sens. 47 (6), 1685–1697.
Gao, Jue, Li, Haisen, Chen, Baowei, Zhou, Tian, Xu, Chao, Du, Weidong, 2017. Fast two-dimensional subset censored CFAR method for multiple objects detection from acoustic image. IET Radar, Sonar Navig. 11 (3), 505–512.
Jung, D., Kim, J., Byun, G., 2018. Numerical modeling and simulation technique in time-domain for multibeam echo sounder. Int. J. Nav. Architect. Ocean. Eng. 10 (2).
Kammerer, Edouard, Sep. 2000. A New Method for the Removal of Refraction Artifacts in Multibeam Echosounder Systems. University of New Brunswick, pp. 35–60.
Kronauge, M., Rohling, H., 2013. Fast two-dimensional CFAR procedure". IEEE Trans. Aero. Electron. Syst. 49 (3), 1817–1823.
Rohling, Hermann, 1983. Radar cfar thresholding in clutter and multiple target situations. IEEE Trans. Aero. Electron. Syst. (4), 608–621P. AES-19.
Tao, DingDoulgeris, Anthony, P., Camilla, Brekke, 2016. A segmentation-based CFAR detection algorithm using truncated statistics. IEEE Trans. Geosci. Rem. Sens. 54 (5), 2887–2898.
Villar, Sebastián A., Acosta, Gerardo G., Senna, André Sousa, Rozenfeld, Alejandro, 2013. Pipeline Detection System from Acoustic Images Utilizing CA-CFAR. Oceans - San Diego.
Villar, Sebastían A., De Paula, Mariano, Solari, Franco J., 2017. A framework for acoustic segmentation using order statistic-constant false alarm rate in two dimensions from sidescan sonar data. IEEE J. Ocean. Eng. 99, 1–14.
Wei, Y.-K., Weng, N.-N., Li, H.-S., Yao, B., Zhou, T., 2010. Eliminating the tunnel effect in multi-beam bathymetry sonar by using the recursive least square-Laguerre lattice algorithm. J. Harbin Eng. Univ. 31 (5), 547–552.
Yukuo, W., Baowei, C., Haisen, L., 2011. Tunnel effect elimination in multibeam bathymetry sonar based on MVDR algorithm. Hydrographic Surveying and Charting 31 (1), 28–31.
YuZhe, F., HaiSen, L., Chao, X., BaoWei, C., Du, WeiDong, 2017. Spatial correlation of underwater bubble clouds based on acoustic scattering. Acta Phys. Sin. 66 (1).